HHS Public Access

Author manuscript

Science. Author manuscript; available in PMC 2017 June 08.

Published in final edited form as:

Science. 2016 December 09; 354(6317): 1278–1282. doi:10.1126/science.aah6837.

Dopamine Neurons Encode Performance Error in Singing Birds

Vikram Gadagkar[1], **Pavel A. Puzerey**[1], **Ruidong Chen**[1], **Eliza Baird-Daniel**[1,2], **Alexander R. Farhang**[1,3], and **Jesse H. Goldberg**[1,*]

[1]Department of Neurobiology and Behavior, Cornell University, Ithaca, NY 14853, USA

Abstract

Many behaviors are learned through trial and error by matching performance to internal goals. Yet neural mechanisms of performance evaluation remain poorly understood. We recorded basal ganglia projecting dopamine neurons in singing zebra finches as we controlled perceived song quality with distorted auditory feedback. Dopamine activity was phasically suppressed after distorted syllables, consistent with a worse-than-predicted outcome, and was phasically activated at the precise moment of the song when a predicted distortion did not occur, consistent with a better-than-predicted outcome. Error response magnitude depended on distortion probability. Thus dopaminergic error signals can evaluate behaviors that are not learned for reward and are instead learned by matching performance outcomes to internal goals.

When practicing piano how do you know if you struck the right or wrong note? The problem is that there is nothing intrinsically 'good' or 'bad' about the sound of A-sharp. It entirely depends if that's the note you *wanted* to strike at that time-step of the song. Performance evaluation requires sensory feedback to be compared with internal benchmarks that change from moment to moment in a sequence. Performance errors during musical performance (1, 2) and speech production (3) are associated with a frontal error-related negativity in the electroencephalogram that may relate to activity in ventral tegmental area (VTA) dopamine neurons (4). Yet while dopamine neurons are known to encode reward prediction error in tasks where animals seek primary rewards such as food or juice (5–7), it is not known if dopamine activity also encodes error in tasks that are not learned for primary reward and are instead learned by matching sensory feedback to internal performance benchmarks (8, 9).

Songbirds use auditory feedback to learn to sing and have a dopaminergic projection from VTA to Area X, a nucleus required for song learning (10–13). It's hypothesized that a singing bird evaluates its own song to compute an auditory-error based reinforcement signal that guides learning – i.e. a neural signal that 'tells' vocal motor circuits if the recent vocalization was 'good' and should be reinforced or 'bad' and be eliminated (14, 15) (Fig.

*Corresponding author. jessehgoldberg@gmail.com.
[2]Current address: Department of Neurological Surgery, Weill Cornell Medical College, New York, NY 10065, USA
[3]Current address: Department of Anatomy, University of California, San Francisco, California 94143, USA

Supplementary Materials:
Materials and Methods
Supplementary Text
Figures S1–S12
Tables S1–S2
Movie S1

1A). The neural correlates of song evaluation remain unknown (16–18), leading to alternative models of learning that do not require online error signals (19).

To test if dopamine activity encodes performance error, we recorded songbird VTA neurons while controlling perceived song quality with distorted auditory feedback (DAF) (18, 20–24) (Fig. 1B to F). Beginning days prior to recordings, a specific song syllable was either distorted with DAF or, on randomly interleaved trials, left undistorted altogether (distortion rate 44 ± 8%, n = 26 birds, Fig. 1, E and F). DAF was a 50 millisecond snippet of sound with the same amplitude and spectral content as normal zebra finch song (see supplementary text). The snippet was either a segment of one of the bird's own syllables displaced in time (displaced-syllable DAF, n = 10 birds, Fig. 1E) or a synthesized sound designed to mimic broadband portions of the bird's own song (broadband DAF, n = 16 birds) (20, 24). Operant broadband DAF drives dopamine and Area X-dependent reinforcement of undistorted syllable variants (13, 23). Displaced-syllable DAF, when operantly delivered contingent on the pitch of a harmonic target syllable, resulted in similar learning (Fig 1G, H) (20).

To test for online error responses, we compared the activity between randomly interleaved renditions of distorted and undistorted songs. We computed the z-scored difference between target onset-aligned distorted and undistorted rate histograms (Fig. 2, A to D, target onset defined as the median DAF onset time relative to distorted syllable onset, n = 125 neurons in 26 birds) (24). We defined the *error response* as the average z-scored difference in firing in a 50–125 millisecond interval following target onset (24). We plotted the distribution of error responses across the 125 VTA neurons and observed two distinct groups: one that did not exhibit significant error responses (n = 108 neurons, error response: 0.1 ± 0.9) and a group of error-responding neurons (n = 17 neurons, error response 3.3 ± 0.5, Fig. 2, E and F) that formed a distinct cluster ($P < 0.001$, bootstrap) (24). These two groups, defined as VTAerror (n = 17) and VTAother (n = 108), were spatially intermingled (fig. S1).

All VTAerror neurons were phasically suppressed by DAF during singing (Fig. 2, A to D, G, $P < 0.05$ in 17/17 VTAerror neurons, bootstrap). Suppressions followed DAF onset with a latency of 58 ± 13 ms, lasted 86 ± 35 ms and resulted on average in a 75% reduction in firing rate (range: 45–100%; (24, 25)). DAF-induced suppressions during singing were highly reliable, occurring on an average of 94% of distorted trials (range: 82–100%). VTAerror neurons also exhibited phasic activations following the precise time-step of undistorted songs where DAF would have occurred but did not occur (Fig. 2, A to D, G, and I, $P < 0.05$ in the same 17 neurons that exhibited suppressions on distorted trials, bootstrap). Phasic activations mirrored the phasic suppressions: they followed target onsets with a latency of 51 ± 20 ms, lasted 62 ± 27 ms and resulted on average in a 77% (range: 42–214%) increase in firing rate (24) (Fig. 2H).

These precisely timed phasic activations suggest that undistorted target syllables are signaled as better than predicted, as if they are evaluated against an estimate of syllable quality that is diminished by a memory of errors (i.e. a flexible performance benchmark, see Supplementary text). To test if error signals are scaled by error history, we trained 10 birds in a two-target paradigm in which one syllable was distorted with a high probability (target 1, 49 ± 4%) and a second syllable with low probability (target 2, 20 ± 4%) (Fig. 3A to C)

(24). The magnitude and reliability of phasic suppressions did not depend on error probability (% suppression: target-1: 59%, range: 45–77%; target-2: 63%, range: 20–100%, reliability: target-1: 90%, range: 82–100%; target-2: 86%, range: 71–100%, $P > 0.4$, rank sum tests, Fig. 3D), consistent with weak scaling of dopaminergic negative reward prediction error responses (6, 7). In contrast, phasic activations were significantly larger following (the more surprising) undistorted renditions of the high probability target (increase in firing rate, target-1: 67%, range: 42–159%; target-2: 22%, range: −3–48%, $P < 0.001$, rank sum test; Fig. 3E). Error responses to target 2 did not depend on whether or not the preceding target 1 was distorted and vice versa, indicating that song time-steps are independently evaluated against temporally aligned performance benchmarks ($P > 0.05$, rank sum tests and fig. S2).

Over 95% of Area X projecting VTA neurons are dopaminergic (11). Fourteen of 125 VTA neurons were antidromically identified as projecting to Area X (Fig. 1B to D), and 13/14 VTAx neurons encoded performance error (Fig. 2E and F). VTAerror neurons discharged like mammalian dopamine neurons (see supplementary text, figs. S3 to S5).

Dopamine activity correlates with movement (26, 27). We quantified movement with microdrive-mounted accelerometers (fig. S6 and Movie S1). The activity of many VTA neurons was modulated by movement, which was in turn correlated with singing. But movement patterns during singing were not affected by DAF and error responses were not affected by movement (n = 26/26 birds, $P > 0.05$, bootstrapped d' analysis, see supplementary text, Table S1 and S2, and figs. S6 to S10).

VTAerror neurons might not encode performance error but simply the presence or absence of DAF as if it were an aversive stimulus (see supplementary text). An aversive response should persist in birds during non-singing periods whereas performance error should be restricted to singing. During non-singing periods VTAerror neurons did not differentially respond to playback of distorted and undistorted renditions of the bird's own song (normalized firing rate, distorted: 1.0 ± 0.2, undistorted: 1.1 ± 0.1, $P > 0.3$, unpaired t-test) (Fig. 4) and did not exhibit pauses in response to DAF (fig. S11). Confinement of VTAerror responses to singing is consistent with performance error.

Performance error signals during singing are similar to prediction error signals during reward seeking (5). Suppression of VTAerror activity after distorted syllables resembles the dopamine response to worse-than-predicted reward outcomes. Activation of VTAerror neurons after undistorted syllables resembles the dopamine response to better-than-predicted reward outcomes. The scaling of positive VTAerror responses according to error history suggests that song is evaluated against flexible performance benchmarks. Positive reward prediction error signals are also scaled by reward prediction (6, 7). Finally, performance and reward prediction error signals could underlie similar learning mechanisms. Dopamine-modulated corticostriatal plasticity links external stimuli to reward-maximizing responses (14). Dopamine-modulated corticostriatal plasticity also exists inside Area X (28) and could similarly link each time-step in the song to the specific vocalization that produces a favorable outcome when produced at that time-step (supplementary text and fig. S12). Such a mechanism would explain the reinforcement of undistorted syllable variants in operant

DAF paradigms (Fig. 1G and H) (18, 20, 21, 23) and could contribute to natural song learning (14).

Yet unlike reward prediction error, performance error during singing is not derived from sensory feedback of intrinsic reward or reward-predicting value. The absence of error responses in birds passively hearing distorted or undistorted syllables suggests that there is nothing intrinsically 'good' or 'bad' about these sounds according to the performance monitoring system. Performance error might instead derive from evaluation of auditory feedback against internal performance benchmarks that require, at each time-step of the song sequence, information about the desired outcome, the actual outcome, and also the predicted probability of achieving the desired outcome. It remains unknown how upstream circuits construct the VTAerror signal. Multiple auditory cortical areas, including one that projects to VTA, respond to DAF specifically during singing (22, 25), providing a candidate pathway for auditory mismatch signals to reach VTA. A newly identified Area X – basal forebrain – VTA pathway (29) might additionally provide a temporally precise and syllable-specific memory of errors required to compute a benchmark against which mismatch error signals are scaled.

Supplementary Material

Refer to Web version on PubMed Central for supplementary material.

Acknowledgments

We thank Joe Fetcho, Melissa Warden, Michael Long, Aaron Andalman, and Dmitriy Aronov for comments on the manuscript; Jeremiah Cohen for mouse VTA recording data; Tejapratap Bollu and Don Murdoch for technical support; Jieying Wu and Kamal Maher for histology; Andrew Treska for art. Funding support to JHG by NIH (grant # R01NS094667), Pew Charitable Trusts and Klingenstein Neuroscience Foundation and to VG by Simons Foundation. VG and JHG designed the research, analyzed the data and wrote the paper. VG, PAP, RC, ARF, EB and JHG performed experiments. The authors declare no competing financial interest. Data can be accessed at http://www.nbb.cornell.edu/goldberg/

References

1. Maidhof C, Vavatzanidis N, Prinz W, Rieger M, Koelsch S. J Cogn Neurosci. Oct.2010 22:2401. [PubMed: 19702473]
2. Katahira K, Abla D, Masuda S, Okanoya K. Neurosci Res. May.2008 61:120. [PubMed: 18359117]
3. Trewartha KM, Phillips NA. Front Hum Neurosci. 2013; 7:763. [PubMed: 24273506]
4. Holroyd CB, Coles MG. Psychol Rev. Oct.2002 109:679. [PubMed: 12374324]
5. Schultz W, Dayan P, Montague PR. Science. Mar 14.1997 275:1593. [PubMed: 9054347]
6. Fiorillo CD, Tobler PN, Schultz W. Science. Mar 21.2003 299:1898. [PubMed: 12649484]
7. Bayer HM, Glimcher PW. Neuron. Jul 7.2005 47:129. [PubMed: 15996553]
8. Wolpert DM, Diedrichsen J, Flanagan JR. Nat Rev Neurosci. Dec.2011 12:739. [PubMed: 22033537]
9. Singh S, Lewis R, Barto A, Sorg J. IEEE TRANSACTIONS ON AUTONOMOUS MENTAL DEVELOPMENT. 2010; 2:70.
10. Konishi M. Z Tierpsychol. Dec.1965 22:770. [PubMed: 5874921]
11. Person AL, Gale SD, Farries MA, Perkel DJ. J Comp Neurol. Jun 10.2008 508:840. [PubMed: 18398825]
12. Scharff C, Nottebohm F. J Neurosci. Sep.1991 11:2896. [PubMed: 1880555]

13. Hoffmann LA, Saravanan V, Wood AN, He L, Sober SJ. J Neurosci. Feb 17.2016 36:2176. [PubMed: 26888928]
14. Fee MS, Goldberg JH. Neuroscience. Dec 15.2011 198:152. [PubMed: 22015923]
15. Doya K, Sejnowski T. Advances in Neural Information Processing Systems. 1995; 7:101.
16. Leonardo A. Proc Natl Acad Sci U S A. Nov 30.2004 101:16935. [PubMed: 15557558]
17. Kozhevnikov AA, Fee MS. J Neurophysiol. Jun.2007 97:4271. [PubMed: 17182906]
18. Hamaguchi K, Tschida KA, Yoon I, Donald BR, Mooney R. Elife. 2014; 3:e01833. [PubMed: 24550254]
19. Hahnloser, R., Ganguli, S. Principles of Neural Coding. Panzeri, S., Quiroga, P., editors. CRC Taylor and Francis; Boca Raton, FL: 2013. p. 547-564.
20. Andalman AS, Fee MS. Proc Natl Acad Sci U S A. Jul 28.2009 106:12518. [PubMed: 19597157]
21. Tumer EC, Brainard MS. Nature. Dec 20.2007 450:1240. [PubMed: 18097411]
22. Keller GB, Hahnloser RH. Nature. Jan 8.2009 457:187. [PubMed: 19005471]
23. Ali F, et al. Neuron. Oct 16.2013 80:494. [PubMed: 24075977]
24. Materials and methods are available as supplementary materials on Science Online.
25. Mandelblat-Cerf Y, Las L, Denisenko N, Fee MS. Elife. 2014:3.
26. Jin X, Costa RM. Nature. Jul 22.2010 466:457. [PubMed: 20651684]
27. Howe MW, Dombeck DA. Nature. Jul 11.2016
28. Ding L, Perkel DJ. J Neurosci. Jan 14.2004 24:488. [PubMed: 14724247]
29. Gale SD, Perkel DJ. The Journal of neuroscience. Jan 20.2010 30:1027. [PubMed: 20089911]
30. Goldberg JH, Fee MS. Journal of Neurophysiology. Apr.2010 103:2002. [PubMed: 20107125]
31. Bayer HM, Lau B, Glimcher PW. J Neurophysiol. Sep.2007 98:1428. [PubMed: 17615124]
32. Goldberg JH, Fee MS. Nature Neuroscience. Apr.2012 15:620. [PubMed: 22327474]
33. Canopoli A, Herbst JA, Hahnloser RH. J Neurosci. May 14.2014 34:7018. [PubMed: 24828654]
34. Charlesworth JD, Warren TL, Brainard MS. Nature. Jun 14.2012 486:251. [PubMed: 22699618]
35. Cynx J. J Comp Psychol. Mar.1990 104:3. [PubMed: 2354628]
36. Horita H, Wada K, Jarvis ED. Eur J Neurosci. Dec.2008 28:2519. [PubMed: 19087177]
37. Akutagawa E, Konishi M. J Comp Neurol. Aug 1.2010 518:3086. [PubMed: 20533361]
38. Ganguli, S., Hahnloser, R. paper presented at the CoSyne; Salt Lake City, UT. February 27 2011;
39. Blakemore SJ, Frith CD, Wolpert DM. J Cogn Neurosci. Sep.1999 11:551. [PubMed: 10511643]
40. West MJ, King AP. Nature. Jul 21.1988 334:244. [PubMed: 3398921]
41. Zann, RA. The zebra finch: a synthesis of field and laboratory studies. Vol. 5. Oxford University Press; 1996.
42. Benichov JI, et al. Curr Biol. Feb 8.2016 26:309. [PubMed: 26774786]
43. Riters LV. Front Neuroendocrinol. Apr.2012 33:194. [PubMed: 22569510]
44. Marler P. J Neurobiol. Nov.1997 33:501. [PubMed: 9369456]
45. Aronov D, Fee MS. PLoS One. 2012; 7:e47856. [PubMed: 23112858]
46. Goldberg JH, Adler A, Bergman H, Fee MS. J Neurosci. May 19.2010 30:7088. [PubMed: 20484651]
47. Gale SD, Perkel DJ. J Neurophysiol. Nov.2006 96:2295. [PubMed: 16870835]
48. Marinelli M, McCutcheon JE. Neuroscience. Dec 12.2014 282:176. [PubMed: 25084048]
49. Lobb CJ, Jaeger D. Neurobiol Dis. Mar.2015 75:177. [PubMed: 25576395]
50. Niv Y, Daw ND, Joel D, Dayan P. Psychopharmacology (Berl). Apr.2007 191:507. [PubMed: 17031711]
51. Cohen JY, Amoroso MW, Uchida N. Elife. 2015; 4
52. Yanagihara S, Hessler NA. Eur J Neurosci. Dec.2006 24:3619. [PubMed: 17229110]
53. Riesel A, Weinberg A, Endrass T, Meyer A, Hajcak G. Biol Psychol. Jul.2013 93:377. [PubMed: 23607999]
54. Simons RF. Psychophysiology. Jan 1.2010 47:1. [PubMed: 19929897]
55. Barter JW, et al. Front Integr Neurosci. 2015; 9:39. [PubMed: 26074791]

56. Romo R, Schultz W. J Neurophysiol. Mar.1990 63:592. [PubMed: 2329363]
57. Sutton, RS., Barto, AG. Reinforcement learning: an introduction. MIT Press; Cambridge, MA: 1998. p. 322
58. Hong S, Hikosaka O. Front Behav Neurosci. 2011; 5:15. [PubMed: 21472026]
59. Kao MH, Doupe AJ, Brainard MS. Nature. Feb 10.2005 433:638. [PubMed: 15703748]
60. Olveczky BP, Andalman AS, Fee MS. PLoS Biol. May.2005 3:e153. [PubMed: 15826219]
61. Hoover JE, Strick PL. Science. Feb 5.1993 259:819. [PubMed: 7679223]
62. Elemans CP. Curr Opin Neurobiol. Oct.2014 28:172. [PubMed: 25171107]
63. Luo M, Ding L, Perkel DJ. J Neurosci. Sep 1.2001 21:6836. [PubMed: 11517271]
64. Gale SD, Person AL, Perkel DJ. J Comp Neurol. Jun 10.2008 508:824. [PubMed: 18398824]
65. Nottebohm F, Kelley DB, Paton JA. J Comp Neurol. Jun 1.1982 207:344. [PubMed: 7119147]
66. Redondo RL, Morris RG. Nature reviews Neuroscience. Jan.2011 12:17. [PubMed: 21170072]
67. Yagishita S, et al. Science. Sep 26.2014 345:1616. [PubMed: 25258080]
68. Fee MS. Front Neural Circuits. 2012; 6:38. [PubMed: 22754501]

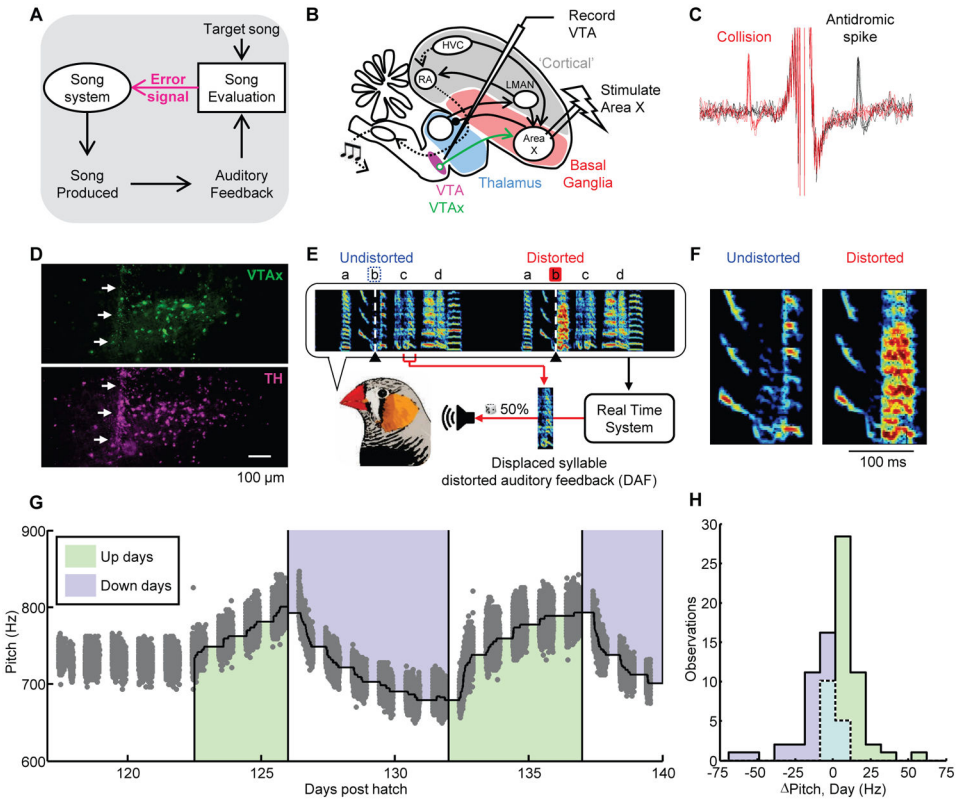

Fig. 1. Experimental test of performance error signals in birdsong

(**A**) Evaluation of auditory feedback during singing is hypothesized to result in 'error' signals that reach the song system. (**B**) Strategy for antidromic identification of VTAx dopamine neurons. (**C**) Antidromic spikes (black) and spike collisions (red) of a VTAx neuron. (**D**) VTAx neurons labeled by injection of retrograde tracer into Area X (green, top) and co-labeled dopamine neurons stained with anti-tyrosine hydroxylase (TH) antibody (purple, bottom). White arrows point to the visible path of the electrode that recorded the VTAx unit shown in Fig. 2A (Scale, 100 µm; anterior-right, dorsal-top). (**E**) Example of displaced-syllable DAF. A snippet of syllable 'c' was played back during production of the target syllable 'b' (Target time, black triangles and white dashed lines). Randomly interleaved target renditions were left undistorted (undistorted trials, blue dashed line). (**F**) Expanded view of the target syllable. **(G)** Pitch-contingent displaced-syllable DAF drives learning. Grey dots denote mean pitch of 49716 target syllable renditions sung over 23 days for one bird. Shading demarcates distorted renditions; green, low pitch variants distorted (up days); blue, high pitch variants distorted (down days). **(H)** Histogram of pitch changes learned during each day (n=4 birds).

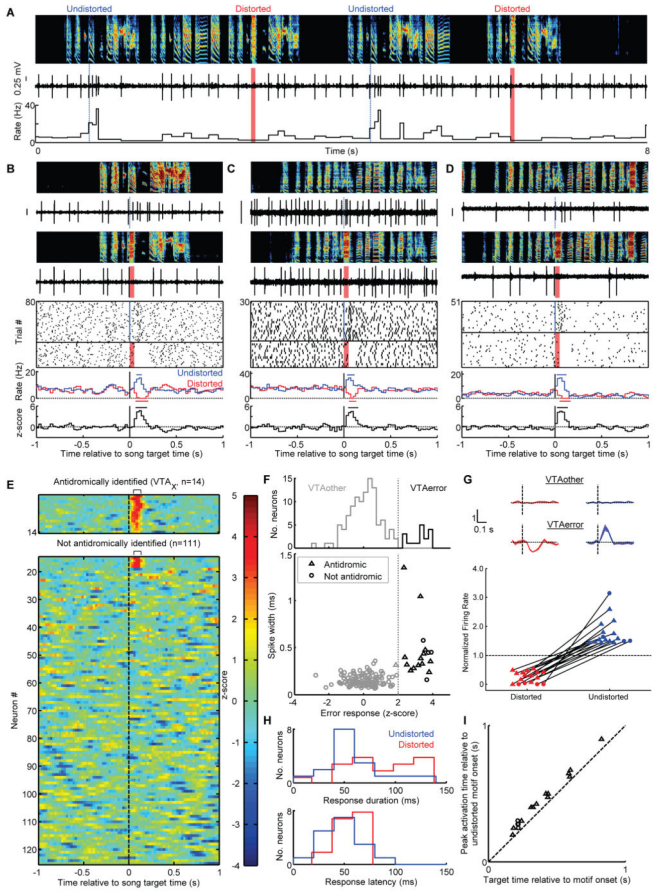

Fig. 2. VTA neurons encode performance error during singing

(A) Spectrogram, voltage trace and the instantaneous firing rate of a VTAx neuron (DAF, red shading; undistorted targets, blue lines). (**B**) Top to bottom: spectrograms, spiking activity during undistorted and distorted trials, corresponding spike raster plots and rate histograms, and z-scored difference between undistorted and distorted rate histograms (plots aligned to target onset). Horizontal bars in histograms indicate significant deviations from baseline ($P <$ 0.05, z-test) (24). (**C**) and (**D**) Two additional VTAerror neurons as in (B). (**E**) Each row plots the z-scored difference between undistorted and distorted target-aligned rate histograms. VTAx neurons (top, n=14) and non-antidromic neurons (bottom, n=111) are independently sorted by maximal z-score. (**F**) Top, distribution of error responses(24). Bottom, spikewidth versus error response (triangles: antidromic, circles: non-antidromic neurons). (**G**) Normalized response to distorted and undistorted targets (mean ± SEM) for VTAother (top) and VTAerror neurons (middle). Bottom, scatterplot of normalized rate in the 50–125 milliseconds following distorted and undistorted trials (solid fills indicate $P <$ 0.05, bootstrap). (**H**) Distributions of phasic response durations (top) and latencies (bottom). (**I**) For each VTAerror neuron, the time of maximal firing rate relative to motif onset is plotted against target time.

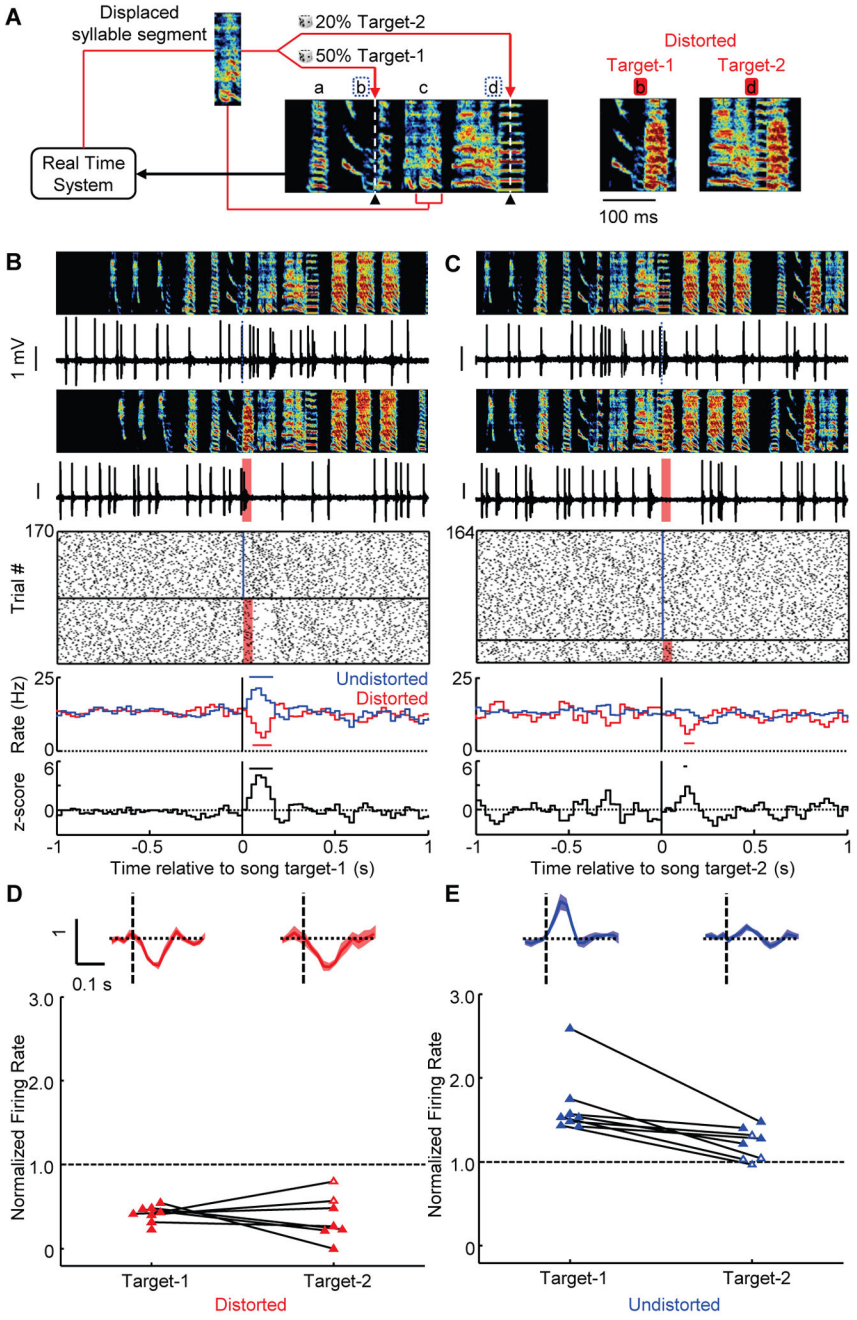

Fig. 3. VTAerror responses depend on error probability

(A) Displaced-syllable DAF scheme with 2 targets per motif (syllable b: target-1, distortion rate: 50%; syllable d, target-2, distortion rate: 20%, target times marked with dashed white line and black triangle). The distorted versions of the two target syllables are shown at right (color scheme as in Fig. 1E). **(B)** Target-1 and **(C)** target-2 error responses for the same neuron. Top to bottom: spectrograms, spiking activity during undistorted and distorted trials, corresponding spike raster plots and rate histograms, and z-scored difference between undistorted and distorted rate histograms (all plots aligned to target onset). Horizontal bars in histograms indicate significant deviations from baseline ($P < 0.05$, z-test) (24). **(D)** Top,

normalized responses to distorted targets (mean ± SEM) for VTAerror neurons. Bottom, scatterplot of normalized rate in the 50–125 milliseconds following target time (solid fills indicate $P < 0.05$, bootstrap). **(E)** Same as (D) but for undistorted targets.

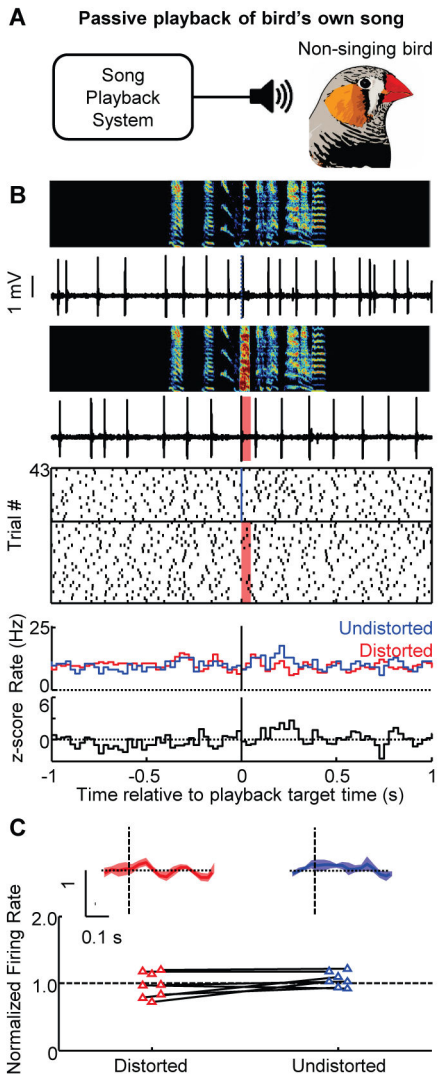

Fig. 4. Response of VTAerror neurons to birdsong during non-singing

(A) Distorted and undistorted renditions of the bird's own song was played back during non-singing periods. **(B)** Top to bottom: spectrograms, spiking activity of the VTAx neuron shown in Fig. 3 during playback of undistorted and distorted songs, corresponding spike raster plots and rate histograms, and z-scored difference between undistorted and distorted rate histograms (all plots aligned to target onset). **(C)** Normalized responses to distorted and undistorted targets (mean ± SEM) for VTAerror neurons during passive playback (top). Bottom, scatterplot of normalized rate in the 50–125 milliseconds following target time (empty fills indicate no significant response, $P > 0.05$, bootstrap) (24)).